symmetry

MDPI

Article

Information Geometry of Evolutionary Dynamics: Fisher–Shahshahani Geometry, Evolutionary Currents, and Response

Angelo Plastino

Physics Department, Universidad Nacional de La Plata, La Plata 1900, Argentina; plastino@fisica.unlp.edu.ar

Abstract

We present a unified information-geometric synthesis of evolutionary dynamics in which population states are represented as probability distributions on a statistical manifold endowed with the Fisher information metric. By separating the kinematic statistical representation of a population from the biological dynamical laws governing its trajectories, the framework treats pure selection, mutation–selection, and non-gradient evolutionary processes within a common geometric setting. We review how the squared Fisher-geometric speed equals the variance of fitness, under pure replicator dynamics and decompose this speed into selection, mutation, and geometric cross-term contributions for general selection–mutation flows. When an evolutionary potential Φ_E exists, the dynamics take the form of a Fisher-natural-gradient flow satisfying a conditional dissipation identity. For general non-gradient evolutionary regimes, such as cyclic frequency-dependent selection, persistent evolutionary currents prevent a global potential formulation, requiring local stability and linear responses to be inferred from the full Jacobian matrix, rather than the Fisher-relative Hessian alone.

Keywords: evolutionary dynamics; fisher geometrty; selection-mutation contributions

1. Introduction

Evolutionary dynamics provides a natural setting in which probabilistic descriptions, dynamical laws, and geometric structures meet. A population can be represented by the frequencies of its different types, and these frequencies form a normalized probability distribution. Selection, mutation, migration, and environmental changes then generate a time-dependent trajectory through the corresponding space of population states. This probabilistic representation suggests that tools developed for the geometry of statistical models provide useful language for describing the evolutionary change, provided that the statistical geometry is clearly distinguished from the biological mechanisms generating the dynamics.

The geometric structure of statistical models is based on the Fisher information metric. The Fisher information metric originated in the theory of statistical estimation and was subsequently given a differential-geometric interpretation as a Riemannian metric on families of probability distributions [1,2]. In modern information geometry, a parametrized statistical model is regarded as a statistical manifold whose local metric measures the distinguishability of nearby probability distributions [3–5]. For a family of distributions $p(x|\theta)$, the Fisher metric is

Check for updates

Academic Editor: Michel Planat

Received: 25 October 2026
Revised: 19 November 2026
Accepted: 25 November 2026
Published: 28 November 2026

Copyright: © 2026 by the author. Licensee MDPI, Basel, Switzerland. This article is an open access article distributed under the terms and conditions of the Creative Commons Attribution (CC BY) license.

$$g_{ab}(\theta) = \mathbb{E}_\theta[\partial_a \log p(X|\theta)\, \partial_b \log p(X|\theta)], \tag{1}$$

and the corresponding infinitesimal statistical distance is

$$ds_F^2 = g_{ab}(\theta)\, d\theta^a d\theta^b. \tag{2}$$

The importance of this construction is that the metric is determined by the statistical model itself, rather than by an arbitrarily chosen Euclidean representation of its parameters [3,4].

In population biology, the simplex of population frequencies provides a particularly important example of such a statistical manifold. In particular, the Shahshahani metric is a Riemannian metric that was introduced in 1979 to study the differential equations of genetic and population dynamics [6]. It fundamentally alters the geometry used to measure distances on a probability simplex, replacing standard flat Euclidean distance with a non-Euclidean structure. Mathematically, in the interior of the probability simplex, it coincides with the Fisher information metric for the categorical distribution, up to a constant normalization convention [6–8]. Let p_i denote the frequency of type i, with

$$p_i \geq 0, \qquad \sum_i p_i = 1; \tag{3}$$

then, the Fisher metric for the corresponding categorical distribution induces the Shahshahani metric on the simplex [6].

This observation establishes a direct connection between information geometry and evolutionary game theory. In particular, the replicator equation

$$\dot{p}_i = p_i(f_i - \bar{f}), \qquad \bar{f} = \sum_j p_j f_j, \tag{4}$$

can be interpreted geometrically in terms of the Shahshahani metric, and in appropriate cases, it possesses a gradient-flow representation [6–8]. More generally, the relationship between the Fisher metric and replicator dynamics provides an information-geometric formulation of natural selection and evolutionary game dynamics [8–11].

A well-known result connects Fisher-geometric speed and the variance of fitness. For the replicator equation, the squared speed of the population trajectory measured with the Fisher metric is

$$v_F^2 = g_{ij}\dot{p}_i\dot{p}_j, \tag{5}$$

and, with the categorical Fisher metric on the simplex, one obtains

$$v_F^2 = \sum_i p_i(f_i - \bar{f})^2 = \mathrm{Var}_p(f). \tag{6}$$

This relation provides a geometric formulation of the connection between variation in fitness and evolutionary change and can be viewed as an information-geometric reformulation of an aspect of Fisher's fundamental theorem of natural selection [10–12]. Importantly, the geometric statement concerns the rate of change generated by selection; it should not be identified without qualification with the total temporal derivative of the mean fitness when the fitness itself depends explicitly on population composition or on the environment.

The Fisher metric, however, specifies a geometry and does not by itself specify an evolutionary law. This distinction is central to the present synthesis. Given a statistical model $p(x|X)$, the Fisher metric determines the local geometry of the space of population states, but the actual trajectory is determined by a vector field

$$\dot{X}^A = F^A(X). \tag{7}$$

Only under additional assumptions can this vector field be represented as a Fisher-natural-gradient flow. If a scalar evolutionary potential $\Phi_E(X)$ exists such that

$$\dot{X}^A = -g^{AB}\partial_B \Phi_E, \tag{8}$$

then the dynamics have a gradient structure with respect to the Fisher geometry. In this special case,

$$-\frac{d\Phi_E}{dt} = g_{AB}\dot{X}^A\dot{X}^B = v_F^2 \geq 0. \tag{9}$$

Thus, the Fisher metric provides the geometric notion of evolutionary speed, while the potential determines a particular dynamic direction on that geometry. Natural-gradient formulations of this type are well established in information geometry and statistical learning theory [5,13].

The distinction becomes essential for evolutionary systems containing processes that cannot be represented globally as gradient flows. Mutation, migration, frequency-dependent interactions, environmental forcing, and other biological mechanisms can introduce non-gradient components into the evolutionary vector field. A useful general decomposition is therefore

$$\dot{X}^A = -g^{AB}\partial_B \Phi_E + J^A, \tag{10}$$

where J^A denotes a non-gradient evolutionary current. The existence of the Fisher metric remains independent of whether such a decomposition is possible. In particular, the metric can characterize statistical distinguishability, even when no global evolutionary potential exists. This distinction also appears in information-geometric treatments of evolutionary game theory, in which gradient and non-gradient evolutionary systems must be separated according to the structure of their fitness landscapes [8,14]. This separation between geometry and dynamics has direct consequences for stability analysis. For a gradient system of the form of Equation (8), local stability can be studied through the Hessian of the evolutionary potential together with the Fisher metric. Defining

$$H_{AB} = \frac{\partial^2 \Phi_E}{\partial X^A \partial X^B}\bigg| X = X^*, \tag{11}$$

the corresponding Fisher-relative linear operator is

$$L^A{}_B = g^{AC}H_{CB}. \tag{12}$$

For a general evolutionary vector field, however, the appropriate local object is the Jacobian

$$J^A_B = \left.\frac{\partial F^A}{\partial X^B}\right|_{X=X^*}. \tag{13}$$

The two constructions coincide only under the additional assumptions associated with the gradient representation. Consequently, a Fisher metric should not be interpreted as automatically defining the stability matrix of an arbitrary evolutionary system. The same distinction is relevant when discussing response and critical behavior. If a local relaxation mode is characterized by an eigenvalue κ, then its characteristic relaxation time scales schematically as

$$\tau \sim \kappa^{-1}, \tag{14}$$

while the corresponding linear response becomes large as κ approaches zero. In an evolutionary context, such softening of a local mode can be associated with slow relaxation or enhanced susceptibility, provided that a dynamical law and a perturbation–response relation are specified. The Fisher metric alone does not establish criticality or determine the relaxation spectrum. The objective of this paper is therefore to organize evolutionary

dynamics within a unified framework in which these levels of description remain explicit. At the geometric level, population states are represented by probability distributions and endowed with the Fisher information metric. At the dynamic level, evolutionary mechanisms determine the vector field governing motion through the statistical manifold. At the special gradient level, a scalar potential allows the evolutionary dynamics to be expressed as a Fisher-natural-gradient flow. This hierarchy makes it possible to distinguish conclusions that follow from statistical geometry from those requiring additional dynamical assumptions. Finally, we emphasize that the appearance of a Fisher metric should not, by itself, be interpreted as establishing a thermodynamic theory. Thermodynamic interpretations require additional structures, such as thermodynamic potentials, conjugate variables, constitutive relations, balance laws, or suitable integrability conditions. The present synthesis takes Fisher geometry as a statistical-geometric structure and shows how it characterizes evolutionary motion, local stability, and response through the hierarchy

$$\boxed{\text{stat. model} \rightarrow \text{Fisher geom.} \rightarrow \text{dynamical law} \rightarrow \text{evolut. response.}} \tag{15}$$

In positioning this synthesis within the existing literature, we emphasize how the Fisher-geometric formulation extends the classical Shahshahani approach beyond discrete categorical frequencies. Although the Shahshahani metric is formulated specifically in the interior of the finite probability simplex Δ^{m-1}, defining the state space as a general statistical manifold $\mathcal{M}_E = p(z|X) : X \in \Theta$ endowed with the Fisher information metric $g_{AB}(X)$ encompasses both discrete frequency models and continuous or parametric population distributions (such as Gaussian trait distributions parameterized by mean and variance) within a single unified hierarchy. At the same time, our primary aim is organizational: rather than claiming priority for individual geometric identities, we establish a clear separation between statistical geometry, biological dynamical laws, and local responses across both gradient and non-gradient regimes.

Scope and Organization of This Paper

Although the individual mathematical ingredients employed here—including the Fisher–Shahshahani metric [6,7], the relation between evolutionary speed and fitness variance [11,12], natural-gradient flows [13], and relative-entropy conservation in cyclic games [14]—are established in the literature, the contribution of this work lies in organizing them into a coherent, multi-level hierarchy that separates statistical geometry from biological dynamics. The structure of this synthesis is organized as follows:

1. *Statistical State Space and Fisher Geometry (Sections 2 and 3):* Population distributions are represented as points on a statistical manifold endowed with the Fisher information metric, establishing coordinate-invariant measures of statistical distance and evolutionary speed, along with the uniqueness properties guaranteed by Chentsov's theorem [15].
2. *Fisher-Natural-Gradient Evolution (Section 4):* Potential-driven dynamics are formulated as the steepest descent with respect to the Fisher metric [13], yielding the conditional dissipation identity $-d\Phi_E/dt = v_F^2$ and showing how non-gradient currents modify potential decay.
3. *Local Stability and Linear Response (Section 5):* Using a Fisher-orthonormal eigenbasis, relaxation times and linear susceptibilities are shown to scale as κ_α^{-1} in gradient regimes, whereas the full Jacobian governs stability in non-gradient systems.
4. *Non-Gradient Cyclic Dynamics and Selection–Mutation Balance (Sections 6–8):* The framework is applied to the cyclic Rock–Paper–Scissors game on Δ^2, general multi-type selection–mutation flows, and an analytically solvable two-type Bernoulli model, followed by a synthesis of scope and extensions (Sections 9 and 10).

https://doi.org/10.3390/sym18121997

2. Fisher's Evolutionary Characterization and the Statistical State Space

2.1. Evolution as a Transformation of Probability Distributions

The mathematical description of evolutionary change begins with the observation that a population can naturally be characterized by a distribution over a set of possible biological states. Depending on the level of description, the elementary outcomes may represent alleles, genotypes, phenotypes, quantitative traits, reproductive strategies, ecological states, or other evolutionarily relevant configurations. Let

$$z \in \mathcal{Z} \tag{16}$$

denote such an outcome, and let

$$p(z|X) \tag{17}$$

denote its probability in a population whose macroscopic evolutionary state is specified by the vector

$$X = (X^1, \dots, X^n) \in \Theta. \tag{18}$$

The admissible family of population distributions is consequently represented by

$$\mathcal{M}_E = \{p(z|X) : X \in \Theta\}, \tag{19}$$

which is referred to as the *evolutionary statistical state space*. Under suitable regularity and identifiability conditions, this space can be endowed with the structure of a smooth statistical manifold. An evolutionary state is not identified merely with the coordinate vector X: the coordinates provide a parametrization of the state, whereas **the probability distribution contains its statistical content**. Evolutionary change is, therefore, represented as the transformation

$$p(z|X) \to p(z|X + dX), \tag{20}$$

so that a continuous evolutionary process corresponds to a curve through a family of probability distributions. For a finite population-state space,

$$\mathcal{Z} = z_1, \dots, z_m, \tag{21}$$

we write

$$p_i(X) = p(z_i|X), \qquad p_i(X) \geq 0, \qquad \sum_{i=1}^{m} p_i(X) = 1. \tag{22}$$

The population frequencies, therefore, belong to the probability simplex. In continuous models, the probabilities p_i are replaced by a probability density with respect to an appropriate reference measure.

2.2. Population States and Evolutionary Coordinates

Let $\Theta \subseteq \mathbb{R}^n$ be an open parameter domain with local coordinates $X = (X^1, \dots, X^n)$, and assume that the mapping $X \longmapsto p(\cdot|X)$ is sufficiently smooth and locally identifiable. Under a smooth reparameterization $X^A = X^A(\widetilde{X})$, the probability distribution is unchanged, $p(z|X) = p(z|X(\widetilde{X}))$, whereas the coordinate components of evolutionary velocity transform as

$$\dot{\widetilde{X}}^a = \frac{\partial \widetilde{X}^a}{\partial X^A} \dot{X}^A. \tag{23}$$

As the numerical magnitude of $\dot{X}^A$ depends on the chosen coordinate chart, an intrinsic measure of evolutionary change must be formulated directly in terms of the statistical model via the Fisher information metric.

2.3. Evolutionary Trajectories as Curves in Statistical State Space

Let $X^A = X^A(t)$ describe a differentiable evolutionary trajectory with time-dependent distribution $p_t(z) = p(z|X(t))$. By the chain rule,

$$\frac{dp_t(z)}{dt} = \partial_A p(z|X(t)), \dot{X}^A = p_t(z), \ell_A(z; X(t)), \dot{X}^A, \tag{24}$$

where $\ell_A(z; X) = \partial_A \log p(z|X)$ denotes the score function. Along the trajectory,

$$\ell_A \dot{X}^A = \frac{d}{dt} \log p(z|X(t)) \tag{25}$$

measures the instantaneous logarithmic deformation of the distribution. Throughout this work, integrals over $\mathcal{Z}$ with respect to dz are understood with respect to the appropriate reference measure—namely, the counting measure (summation over $z \in \mathcal{Z}$) for discrete state spaces and the Lebesgue measure for continuous trait spaces. Differentiating the normalization condition $\int_{\mathcal{Z}} p(z|X), dz = 1$ under standard regularity conditions yields the zero-mean score identity

$$\mathbb{E}_X[\ell_A] = 0. \tag{26}$$

2.4. Kinematic and Dynamical Questions

The statistical representation separates two logically distinct questions:

1. *Kinematic (geometric):* How distinguishable are two neighboring population states? This is answered by the Fisher information metric.
2. *Dynamical:* Which direction and velocity do the population actually follow? This requires an evolutionary dynamical law.

In particular, the presence of a Riemannian structure does not imply that biological trajectories are geodesics: geodesics are determined by the metric and its Levi–Civita connection, whereas evolutionary trajectories are governed by the biological vector field. Accordingly,

$$\boxed{\text{statistical state space} \quad \neq \quad \text{evolutionary dynamics.}} \tag{27}$$

2.5. From Evolutionary State Space to Fisher Geometry

For a regular statistical model, local distinguishability is measured by the Fisher information matrix

$$g_{AB}(X) = \mathbb{E}X[\partial_A \log p(z|X), \partial_B \log p(z|X)], \tag{28}$$

with line element $ds_F^2 = g_{AB}(X), dX^A dX^B$. For an evolutionary trajectory $X(t)$, the squared Fisher-geometric speed is

$$v_F^2 = g_{AB}(X)\dot{X}^A\dot{X}^B = \mathbb{E}X\left[\left(\frac{d}{dt}\log p(z|X(t))\right)^2\right], \tag{29}$$

and the accumulated Fisher length of a trajectory γ over $[t_0, t_1]$ is

$$L_F[\gamma] = \int {t_0}^{t_1} \sqrt{g_{AB}(X(t))\dot{X}^A(t)\dot{X}^B(t)}, dt. \tag{30}$$

This construction is summarized by

$$\boxed{\text{population state} \rightarrow \text{evol. stat. state space} \rightarrow \text{Fisher geometry.}} \tag{31}$$

3. Fisher Information Geometry and Local Evolutionary Distinguishability

3.1. The Fisher Metric as an Intrinsic Metric on Population States

On the evolutionary statistical manifold $\mathcal{M}_E = p(z|X) : X \in \Theta$, the Fisher information metric [1–4] is given by

$$g_{AB}(X) = \mathbb{E}X[\partial_A \log p(z|X), \partial_B \log p(z|X)], \qquad ds_F^2 = g_{AB}(X), dX^A dX^B. \tag{32}$$

Under standard regularity and local identifiability conditions, $g_{AB}(X)$ is a positive definite on the tangent space, defining a Riemannian metric on the regular part of $\mathcal{M}_E$ that is invariant under smooth reparameterizations.

3.2. Score Representation

In terms of the score functions $\ell_A(z; X) = \partial_A \log p(z|X)$, which satisfy $\mathbb{E}X[\ell_A] = 0$, the Fisher metric equals the covariance matrix of the score:

$$g_{AB} = \mathbb{E}X[\ell_A \ell_B] = \mathrm{Cov}\, X(\ell_A, \ell_B). \tag{33}$$

3.3. Local Statistical Distinguishability and Relative Entropy

For two neighboring distributions $p(z|X)$ and $p(z|X + dX)$, the Kullback–Leibler divergence

$$D_{\mathrm{KL}}(p(z|X)|p(z|X + dX)) = \int_{\mathcal{Z}} p(z|X) \log \frac{p(z|X)}{p(z|X + dX)}, dz \tag{34}$$

expands around $dX = 0$ as

$$D_{\mathrm{KL}}(p(z|X)|p(z|X + dX)) = \frac{1}{2} g_{AB}(X), dX^A dX^B + O(|dX|^3) = \frac{1}{2} ds_F^2 + O(|dX|^3). \tag{35}$$

The Fisher metric thus forms the universal quadratic part of local relative-entropy distinguishability.

3.4. Fisher Metric on the Probability Simplex

When a population consists of m discrete types with frequencies $p_i > 0$ satisfying $\sum_{i=1}^m p_i = 1$, the interior of the probability simplex is

$$\Delta^{m-1} = \left\{ (p_1, \ldots, p_m) : p_i > 0, \ \sum_{i=1}^m p_i = 1 \right\}. \tag{36}$$

A categorical probability distribution describes a discrete random variable taking one of m mutually exclusive states with probabilities $p(z = i) = p_i$. For this distribution, the Fisher line element takes the form

$$ds_F^2 = \sum_{i=1}^m \frac{dp_i^2}{p_i}, \qquad \sum_{i=1}^m dp_i = 0. \tag{37}$$

Equation (37) is the Fisher–Shahshahani metric on the population simplex [6–8]. By Chentsov's theorem [4,15], this metric is uniquely characterized (up to a positive constant normalization factor) by its behavior under Markov morphisms: it is monotone (non-increasing) under general stochastic coarse-graining maps and strictly invariant under congruent embeddings (sufficient statistics). In evolutionary terms, lumping fine-grained alleles into coarse phenotypic classes cannot artificially increase statistical distinguishability, whereas subdividing types into neutral sub-categories preserves ds_F^2 exactly. The singular behavior of Equation (37) at $p_i = 0$ reflects the boundary of the simplex where the statistical model changes rank; our differential-geometric analysis applies to the regular interior Δ^{m-1}.

3.5. Bernoulli Population as a One-Dimensional Example

For a two-type population ($m = 2$) with $p(1|\theta) = \theta$ and $p(0|\theta) = 1 - \theta$ ($0 < \theta < 1$), the Bernoulli distribution is

$$p(x|\theta) = \theta^x (1-\theta)^{1-x}, \qquad x \in 0, 1. \tag{38}$$

The score is $\partial_\theta \log p(x|\theta) = \frac{x}{\theta} - \frac{1-x}{1-\theta}$, yielding the Fisher information and line element

$$g_{\theta\theta} = \frac{1}{\theta(1-\theta)}, \qquad ds_F^2 = \frac{d\theta^2}{\theta(1-\theta)}. \tag{39}$$

Under the coordinate transformation $u = 2\arcsin\sqrt{\theta}$, we have $du = d\theta/\sqrt{\theta(1-\theta)}$, so the line element becomes Euclidean on $0 < u < \pi$:

$$ds_F^2 = du^2, \qquad v_F^2 = \frac{\dot{\theta}^2}{\theta(1-\theta)} = \dot{u}^2. \tag{40}$$

Although the metric is flat in the u coordinate, the evolutionary speed v_F^2 along a trajectory depends on the dynamical law: under pure replicator selection $\dot{\theta} = s, \theta(1-\theta)$, one has $v_F^2 = s^2\theta(1-\theta) = \frac{s^2}{4}\sin^2 u$, which varies across the manifold (Figure 1).

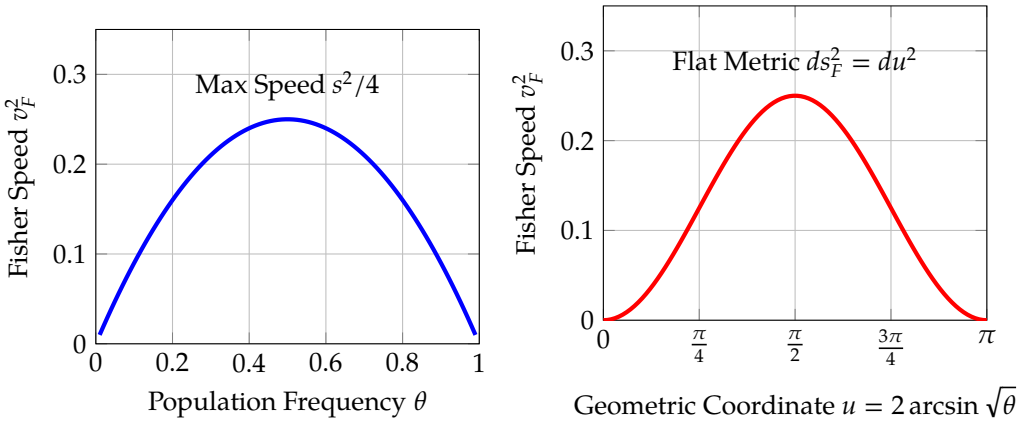

(**a**) (**b**)

Figure 1. Reparameterization invariance on the Bernoulli population manifold for pure replicator dynamics $\dot{\theta} = s, \theta(1-\theta)$ with selection parameter $s = 1$. Although the metric becomes Euclidean ($ds_F^2 = du^2$) in the Fisher coordinate $u = 2\arcsin\sqrt{\theta}$, the squared Fisher speed $v_F^2 = \dot{u}^2 = \frac{s^2}{4}\sin^2 u$ remains state-dependent. (**a**) Speed profile in raw frequency θ ($s = 1$); (**b**) Speed profile in flat Fisher coordinate u ($s = 1$).

3.6. Fisher Geometry and Evolutionary Dynamics

For a general evolutionary system $\dot{X}^A = F^A(X)$, the Fisher metric characterizes the statistical state space, whereas biological mechanisms determine the vector field $F^A(X)$:

$$\boxed{\text{Fisher geometry} \neq \text{evolutionary dynamics.}} \tag{41}$$

4. Fisher-Natural-Gradient Evolution and Local Optimality

4.1. Evolutionary Potentials and Gradient Dynamics

Suppose an evolutionary process on (M_E, g_{AB}) admits a scalar evolutionary potential $\Phi_E(X)$. Recall that the differential $d\Phi_E$ is a covariant one-form with components $\partial_A \Phi_E$, whereas the evolutionary velocity $\dot{X}^A$ is a contravariant tangent vector. Raising the index with the inverse Fisher metric g^{AB} ($g^{AC}g_{CB} = \delta^A_B$) defines the Fisher-natural-gradient dynamics [13]:

$$\dot{X}^A = -g^{AB}(X), \partial_B \Phi_E = -\operatorname{grad}_F \Phi_E. \tag{42}$$

4.2. Local Steepest Descent in Fisher Geometry

Consider a small displacement $X^A \to X^A + dX^A$. Minimizing the first-order potential change $d\Phi_E = \partial_A \Phi_E, dX^A$ subject to a fixed squared Fisher distance $ds_F^2 = g_{AB}, dX^A dX^B = \delta s^2$ via the Lagrangian [13]

$$\mathcal{L} = \partial_A \Phi_E, dX^A + \frac{\lambda}{2}\left(g_{AB}, dX^A dX^B - \delta s^2\right) \tag{43}$$

yields $\partial_A \Phi_E + \lambda g_{AB} dX^B = 0$, or

$$dX^A = -\frac{1}{\lambda} g^{AB} \partial_B \Phi_E. \tag{44}$$

Thus, Equation (42) realizes the local steepest descent with respect to statistical distinguishability.

4.3. Dissipation Identity and Fisher Speed

Along a Fisher-natural-gradient trajectory, the potential evolves according to

$$\frac{d\Phi_E}{dt} = \partial_A \Phi_E \dot{X}^A = -\partial_A \Phi_E g^{AB} \partial_B \Phi_E \leq 0. \tag{45}$$

As $v_F^2 = g_{AB} \dot{X}^A \dot{X}^B = g^{CD} \partial_C \Phi_E \partial_D \Phi_E$, one obtains the conditional dissipation identity

$$-\frac{d\Phi_E}{dt} = v_F^2. \tag{46}$$

This identity holds specifically for Fisher-natural-gradient flows, and is not a general property of arbitrary vector fields on a Fisher manifold.

4.4. Stationary States and Local Optimality

At an interior stationary state X^* ($\dot{X}^A(X^*) = 0$) where $g_{AB}(X^*)$ is nonsingular, Equation (42) implies $\partial_A \Phi_E(X^*) = 0$. Expanding $\Phi_E(X^* + \xi)$ to second-order with Hessian $H_{AB} = \partial_A \partial_B \Phi_E|_{X^*}$ gives the linearized dynamics

$$\dot{\xi}^A = -L^A_{\ B} \xi^B, \qquad L^A_{\ B} = g_*^{AC} H_{CB}, \tag{47}$$

where $L^A_{\ B}$ is the Fisher-relative Hessian. Its eigenmodes satisfy the generalized eigenvalue problem

$$H_{AB} v^B = \kappa g_{AB} v^B \iff L^A_{\ B} v^B = \kappa v^A. \tag{48}$$

For a locally stable minimum ($\kappa > 0$), perturbations decay as $\xi(t) \sim e^{-\kappa t}$ with characteristic relaxation time $\tau \sim \kappa^{-1}$.

4.5. Fisher-Geometric Local Optimality

For finite local displacements $X \to X + \Delta X$, the quadratic Fisher cost $\ell_F^2 = g_{AB}(X) \Delta X^A \Delta X^B$ measures statistical distinguishability, whereas the potential determines the dynamically selected descent direction. Hence, Fisher cost $\neq$ selection rule without specifying a dynamical principle.

4.6. Relation to Replicator Dynamics

In the interior of the probability simplex equipped with the Fisher–Shahshahani metric, potential-driven replicator dynamics take the form $\dot{p}_i = -g^{ij} \partial_j \Phi_E$ (subject to $\sum_i \dot{p}_i = 0$) when the fitness landscape satisfies the appropriate gradient integrability conditions [6–8]. For the two-type replicator equation $\dot{p} = s, p(1-p)$, choosing $\Phi_E(p) = -sp$ yields $\dot{p} = -p(1-p)(-s) = s, p(1-p)$ and $-d\Phi_E/dt = v_F^2 = s^2 p(1-p) = \mathrm{Var}_p(f)$.

4.7. Dissipation Identity and Non-Gradient Currents

When a general evolutionary vector field is decomposed into a Fisher-natural-gradient component and a non-gradient evolutionary current J^A,

$$\dot{X}^A = -g^{AB}\partial_B\Phi_E + J^A, \tag{49}$$

let $v^2_{\text{grad}} = g^{AB}\partial_A\Phi_E\partial_B\Phi_E$ denote the isolated gradient-driven informational speed. The total squared Fisher speed is

$$v_F^2 = g_{AB}\dot{X}^A\dot{X}^B = v^2_{\text{grad}} - 2\partial_A\Phi_E J^A + |J|F^2, \tag{50}$$

where $|J|F^2 = g_{AB}J^AJ^B$. Differentiating Φ_E along the true trajectory yields the exact dissipation relation

$$\frac{d\Phi_E}{dt} = \partial_A\Phi_E\dot{X}^A = -v\text{grad}^2 + \partial_A\Phi_E J^A = -v_F^2 - \partial_A\Phi_E J^A + |J|_F^2. \tag{51}$$

Thus, $-d\Phi_E/dt = v_F^2$ breaks down whenever $J^A \neq 0$: persistent currents can slow or even reverse the decrease of Φ_E depending on the alignment $\partial_A\Phi_E J^A$.

5. Local Stability, Relaxation, and Evolutionary Response

5.1. Stationary Evolutionary States

For a general evolutionary system $\dot{X}^A = F^A(X)$ near a stationary state X^* ($F^A(X^*) = 0$), setting $X^A = X^{A*} + \xi^A$ yields the linearized system

$$\dot{\xi}^A = J^A_B\xi^B + O(|\xi|^2), \qquad J^A_B = \left.\frac{\partial F^A}{\partial X^B}\right| X = X^*. \tag{52}$$

Although the eigenvalues of the Jacobian $J^A\ B$ govern temporal stability, the Fisher metric determines the statistical magnitude of perturbations via $|\xi|F^2 = g_{AB}(X^*)\xi^A\xi^B$.

5.2. Stability in Fisher-Natural-Gradient Dynamics

For Fisher-natural-gradient dynamics $\dot{X}^A = -g^{AB}\partial_B\Phi_E$, linearizing around a stationary point $\partial_A\Phi_E(X^*) = 0$ gives

$$\dot{\xi}^A = -g^{AB}_* H_{BC}\xi^C = -L^A_B\xi^B, \tag{53}$$

where $g^{AB}_* = g^{AB}(X^*)$ and $H_{AB} = \partial_A\partial_B\Phi_E|_{X^*}$. Perturbations along an eigenmode $H_{AB}v^B = \kappa g_{AB}v^B$ with $\kappa > 0$ decay as $\xi_\kappa(t) = \xi_\kappa(0)e^{-\kappa t}$ with relaxation time $\tau_\kappa \sim \kappa^{-1}$.

5.3. Statistically Orthogonal Modes and Linear Evolutionary Response

To evaluate local linear responses in a coordinate-invariant manner, we normalize the generalized eigenvectors $\{v_\alpha\}$ of $H_{AB}v^B_\alpha = \kappa_\alpha g_{AB}v^B_\alpha$ relative to the Fisher metric at X^*:

$$g_{AB}v^A_\alpha v^B_\beta = \delta_{\alpha\beta}. \tag{54}$$

Under this Fisher-orthonormal eigenbasis, the inverse Hessian admits the spectral expansion

$$(H^{-1})^{AB} = \sum_\alpha \kappa_\alpha^{-1}v^A_\alpha v^B_\alpha. \tag{55}$$

Consider a small static environmental or selective perturbation h_A coupled linearly to the coordinates via

$$\Phi_E(X;h) = \Phi_E(X;0) - h_AX^A. \tag{56}$$

Expanding the perturbed stationarity condition $\partial_A \Phi_E(X^*; h) = 0$ to first order yields the linear response mapping

$$H_{AB}\delta X^B = \delta h_A \implies \delta X^A = (H^{-1})^{AB}\delta h_B, \tag{57}$$

whenever H_{AB} is invertible. Although Equation (57) is independent of the metric in coordinate form, the Fisher metric enters directly when decomposing the displacement into statistically orthogonal modes and measuring its invariant statistical length $\delta s_F^2 = g_{AB}(X^*)\delta X^A \delta X^B$. Substituting Equation (55) into Equation (57), the isolated response amplitude χ_α along mode α satisfies

$$\chi_\alpha \equiv |\delta X_\alpha|_g = \kappa\alpha^{-1}|v_\alpha^B \delta h_B| \sim \frac{1}{\kappa_\alpha}. \tag{58}$$

Thus, under linear-response assumptions, both the characteristic relaxation time $\tau_\alpha \sim \kappa_\alpha^{-1}$ and modal susceptibility $\chi_\alpha \sim \kappa_\alpha^{-1}$ scale with the inverse of the same generalized eigenvalue:

$$\tau_\alpha \sim \frac{1}{\kappa_\alpha}, \qquad \chi_\alpha \sim \frac{1}{\kappa_\alpha}. \tag{59}$$

A mode with small generalized curvature ($\kappa_\alpha \to 0$) flattens locally relative to the Fisher metric, exhibiting both slow relaxation and an amplified response—a regime we term *Fisher-geometric softening*. This decomposition cleanly separates (1) the statistical geometry g_{AB}, (2) the local restoring structure H_{AB}, and (3) the dynamical relaxation rates κ_α. Note that these scaling relations are local linear results and do not by themselves establish global stability or a thermodynamic phase transition.

5.4. General Evolutionary Dynamics and the Full Jacobian

When $F^A = -g^{AB}\partial_B \Phi_E + J^A_{\text{ng}}$ contains non-gradient mechanisms, the full Jacobian at X^* is

$$J^A_B = -\frac{\partial}{\partial X^B}\left(g^{AC}\partial_C \Phi_E\right)\Big|_{X^*} + \frac{\partial J^A_{\text{ng}}}{\partial X^B}\Big|_{X^*}, \tag{60}$$

so local stability and response cannot be inferred from g_{AB} and H_{AB} alone.

6. Non-Gradient Currents in Multi-Dimensional Spaces: The Cyclic Rock–Paper–Scissors Game

To demonstrate the necessity of separating statistical geometry from potential-driven dynamics on manifolds of dimensions greater than one, we investigated a cyclic Rock–Paper–Scissors replicator system in the interior of the two-dimensional probability simplex $\Delta^2 = (p_1, p_2, p_3) : p_i > 0, \sum_{i=1}^3 p_i = 1$. Let the antisymmetric zero-sum payoff matrix be given by

$$W = \begin{pmatrix} 0 & -1 & 1 \\ 1 & 0 & -1 \\ -1 & 1 & 0 \end{pmatrix}. \tag{61}$$

The population dynamics are governed by the replicator equations $\dot{p}_i = p_i(f_i - \bar{f})$, where $f_i = \sum_j Wijp_j$ and $\bar{f} = \sum_{j,k} p_j W_{jk} p_k = 0$. This system admits a unique interior stationary point at the barycenter $p^* = (1/3, 1/3, 1/3)$. Linearizing the replicator vector field in the three ambient coordinates around p^* yields

$$J_{ij} = \frac{\partial \dot{p}_i}{\partial p_j}\Big| p^* = \frac{1}{3}\begin{pmatrix} 0 & -1 & 1 \\ 1 & 0 & -1 \\ -1 & 1 & 0 \end{pmatrix}, \tag{62}$$

which possesses a zero eigenvalue associated with the direction normal to the simplex ($\sum_i p_i = 1$). Restricting J_{ij} to the two-dimensional tangent space of the simplex ($\sum_i \delta p_i = 0$) yields purely imaginary eigenvalues $\lambda_\pm = \pm\frac{i}{\sqrt{3}}$. As noted in Section 5, purely imaginary

eigenvalues indicate neutral linear oscillations and do not by themselves establish nonlinear orbital stability. Instead, the existence of closed, undamped periodic orbits is rigorously established through the Kullback–Leibler divergence relative to the barycenter,

$$D_{\mathrm{KL}}(p^* \,\|\, p(t)) = \sum_{i=1}^{3} p_i^* \ln \frac{p_i^*}{p_i(t)} = -\frac{1}{3}\sum_{i=1}^{3} \ln\big(3p_i(t)\big), \tag{63}$$

which is an exact constant of the motion ($\frac{d}{dt}D_{\mathrm{KL}} = 0$) whose level sets form closed curves surrounding p^* [14] (Figure 2). Crucially, as the payoff matrix W is antisymmetric, it violates the symmetry (integrability) condition required for a replicator field to be representable as a Shahshahani gradient flow [6,14] (moreover, a gradient flow cannot possess nontrivial periodic orbits). Consequently, no scalar evolutionary potential Φ_E exists, and the Fisher-relative Hessian H_{AB} and its generalized eigenvalues κ are undefined. The dynamics are driven entirely by a persistent non-gradient evolutionary current $J_i = \dot{p}_i$, producing cyclic probability circulation on Δ^2. Equipped with the Fisher–Shahshahani metric $ds_F^2 = \sum_{i=1}^{3} \frac{dp_i^2}{p_i}$, the squared Fisher speed vanishes at the barycenter p^* (where $f_i = \bar{f} = 0$) and remains strictly positive throughout the remainder of the interior domain ($p \in \Delta^2 \setminus p^*$):

$$v_F^2 = \sum_{i=1}^{3} \frac{\dot{p}_i^2}{p_i} = \sum_{i=1}^{3} p_i(f_i - \bar{f})^2 = \mathrm{Var}_p(f) > 0 \qquad (p \neq p^*). \tag{64}$$

This example confirms that Fisher geometry quantifies statistical distinguishability and evolutionary speed, even when potential dissipation is entirely absent.

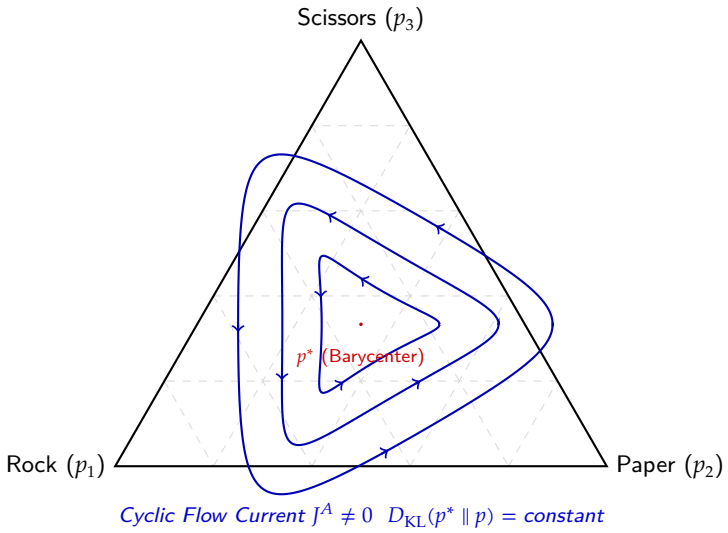

Figure 2. Ternary phase portrait of cyclic Rock–Paper–Scissors replicator dynamics on Δ^2. Trajectories follow closed level sets of constant Kullback–Leibler divergence $D_{\mathrm{KL}}(p^* \,\|\, p)$ around the barycenter $p^* = (1/3, 1/3, 1/3)$, sustained by a non-gradient evolutionary current with $v_F^2 > 0$ for all $p \neq p^*$.

Non-Geodesic Trajectories in Frequency-Dependent Selection

To illustrate explicitly why frequency-dependent evolutionary trajectories generally deviate from Fisher–Shahshahani geodesics, consider a perturbed cyclic Rock–Paper–Scissors game on Δ^2 with payoff matrix

$$W(\epsilon) = \begin{pmatrix} 0 & -1 & 1+\epsilon \\ 1+\epsilon & 0 & -1 \\ -1 & 1+\epsilon & 0 \end{pmatrix}, \tag{65}$$

where $\epsilon \neq 0$ introduces dissipative frequency-dependent selection ($\bar{f}(p) = \epsilon(p_1p_2 + p_2p_3 + p_3p_1) \neq 0$). For $\epsilon = -0.45$, the barycenter $p^* = (1/3, 1/3, 1/3)$ becomes an asymptotically

stable spiral sink with tangent-space Jacobian eigenvalues $\lambda_{\pm} = \frac{\epsilon}{6} \pm \frac{i}{2\sqrt{3}}(2+\epsilon)$, so trajectories spiral inward rather than conserving $D_{\mathrm{KL}}(p^* \,\|\, p)$. In contrast, under the isometric coordinate map $s_i = 2\sqrt{p_i}$ ($\sum_{i=1}^3 s_i^2 = 4$), the Fisher–Shahshahani metric $ds_F^2 = \sum_{i=1}^3 ds_i^2$ maps Δ^2 onto the positive octant of a sphere of radius 2, so Fisher geodesics are great-circle arcs minimizing statistical length $L_F = 2\arccos\left(\sum_{i=1}^3 \sqrt{p_i(0)p_i(T)}\right)$. As shown in Figure 3, the true frequency-dependent trajectory spirals around p^*, accumulating far greater Fisher length than the geodesic connecting its initial and final states.

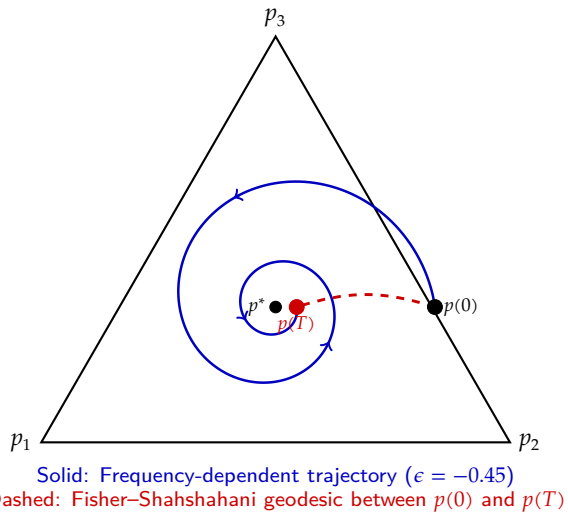

Figure 3. Non-geodesic evolutionary trajectory under frequency-dependent selection on Δ^2. For the asymmetric payoff matrix $W(\epsilon)$ with $\epsilon = -0.45$, the replicator trajectory (solid blue) spirals inward toward the barycenter p^*, deviating substantially from the shortest-path Fisher–Shahshahani geodesic (dashed red) connecting the same endpoints $p(0)$ and $p(T)$.

7. Selection, Mutation, and Non-Gradient Evolutionary Dynamics

7.1. General Selection–Mutation Dynamics and Fisher Speed

For m discrete types on the simplex Δ^{m-1} equipped with $ds_F^2 = \sum_{i=1}^m dp_i^2/p_i$, consider the selection–mutation equation

$$\dot{p}_i = p_i(f_i - \bar{f}) + M_i(p) = F_i^{\mathrm{sel}} + F_i^{\mathrm{mut}}, \qquad \sum_{i=1}^m M_i(p) = 0, \tag{66}$$

where $\bar{f} = \sum_{i=1}^m p_i f_i$. Substituting Equation (66) into $v_F^2 = \sum_{i=1}^m \dot{p}_i^2/p_i$ yields

$$v_F^2 = \mathrm{Var}\, p(f) + 2\sum_{i=1}^m (f_i - \bar{f})M_i + \sum_{i=1}^m \frac{M_i^2}{p_i}, \tag{67}$$

where the mean-fitness contribution to the cross term vanishes because $\sum_i \bar{f} M_i = \bar{f}\sum_i M_i = 0$. The cross term $2g_{ij}F_{\mathrm{sel}}^i F_{\mathrm{mut}}^j$ measures the local Fisher-geometric alignment between selection and mutation, recovering $v_F^2 = \mathrm{Var}_p(f)$ strictly in the pure-selection limit $M_i = 0$.

7.2. Mutation–Selection Balance and Gradient Structure

At an interior stationary distribution p^* ($\dot{p}_i = 0$), the Fisher speed vanishes ($v_F^2(p^*) = 0$), even though the individual selection and mutation currents balance with opposite signs:

$$F_i^{\mathrm{sel}}(p^*) = -F_i^{\mathrm{mut}}(p^*). \tag{68}$$

Whether mutation introduces a genuinely non-gradient component depends on the structure of the transition rates: as shown by Hofbauer [16], when mutation rates depend

solely on the destination type ($M_i(p) = \mu_i - p_i \sum_j \mu_j$), the selection–mutation equation still admits a Shahshahani potential, whereas general asymmetric mutation matrices generate non-gradient currents. In the general case $\dot{X}^A = -g^{AB}\partial_B \Phi_E + J^A_{\mathrm{ng}}$, potential evolution satisfies

$$\frac{d\Phi_E}{dt} = -v^2_{\mathrm{grad}} + \partial_A \Phi_E J^A_{\mathrm{ng}}, \tag{69}$$

and local stability around p^* is determined by the eigenvalues of the full Jacobian $J_{ij} = \partial \dot{p}_i / \partial p_j|_{p^*}$ restricted to $\sum_i \xi_i = 0$, whereas $\delta s^2_F = \sum_i \xi_i^2 / p_i^*$ quantifies perturbation magnitude.

8. Two-Type Selection–Mutation Model: Equilibrium and Relaxation

To illustrate the framework analytically in one dimension, consider a population of two competing types ($\mathrm{m} = 2$) with frequencies $\mathrm{p}_1 = \theta$ and $\mathrm{p}_0 = 1 - \theta$ on the open interval $\theta \in (0,1)$, equipped with the Bernoulli Fisher metric $g_{\theta\theta}(\theta) = [\theta(1-\theta)]^{-1}$. Let $\Delta = \mathrm{f}_1 - \mathrm{f}_0$ denote the selection coefficient and $\mu > 0$ denote a symmetric mutation rate between the two types. The selection–mutation differential equation is

$$\dot{\theta} = F(\theta) = \theta(1-\theta)\Delta + \mu(1-2\theta), \tag{70}$$

where $F^{\mathrm{sel}}(\theta) = \theta(1-\theta)\Delta$ and $F^{\mathrm{mut}}(\theta) = \mu(1-2\theta)$. Inserting Equation (70) into $v_F^2 = g_{\theta\theta}\dot{\theta}^2$ yields

$$v_F^2 = \mathrm{Var}_p(f) + 2\mu(1-2\theta)\Delta + \frac{\mu^2(1-2\theta)^2}{\theta(1-\theta)}, \tag{71}$$

which decomposes the squared Fisher speed into the fitness variance, the pure mutation contribution, and their geometric cross term. Note that, in one dimension, every smooth interior vector field $\mathrm{F}(\theta)$ on (0,1) can be expressed as a Fisher-natural gradient by integrating $\Phi_E(\theta) = -\int \frac{F(\theta)}{\theta(1-\theta)}\, d\theta = -\Delta\theta - \mu \ln[\theta(1-\theta)]$; genuine non-gradient currents therefore require manifolds of dimension two or higher, as in Section 6. At an interior stationary state $\theta^* \in (0,1)$, the net vector field vanishes ($F(\theta^*) = 0$), corresponding to a balance between opposing selection and mutation currents:

$$\theta^*(1-\theta^*)\Delta = -\mu(1-2\theta^*) \implies \Delta = \frac{\mu(2\theta^* - 1)}{\theta^*(1-\theta^*)}. \tag{72}$$

For any $\mu > 0$ and finite Δ, $\mathrm{F}(0) = \mu > 0$ and $\mathrm{F}(1) = -\mu < 0$, whereas $\mathrm{F}''(\theta) = -2\Delta$ is monotonic on (0,1); hence, there exists a unique interior equilibrium $\theta^* \in (0,1)$ that is globally asymptotically stable on (0,1). Linearizing Equation (70) around θ^* gives the Jacobian eigenvalue (which coincides with the negative Fisher-relative Hessian eigenvalue $-\kappa$ in one dimension)

$$J = \left.\frac{d\dot{\theta}}{d\theta}\right|_{\theta^*} = \Delta(1-2\theta^*) - 2\mu. \tag{73}$$

Substituting Equation (72) into J yields the relaxation rate $\kappa = -\mathrm{J}$:

$$\kappa(\theta^*) = \mu\left[\frac{1}{\theta^*(1-\theta^*)} - 2\right] = \mu\,\frac{\theta^{*2} + (1-\theta^*)^2}{\theta^*(1-\theta^*)} > 0. \tag{74}$$

Differentiating $\kappa(\theta^*)$ shows that the relaxation rate attains its minimum at $\theta^* = 1/2$ (where $\Delta = 0$ and the dynamics reduce to pure mutation), with

$$\kappa_{\min} = 2\mu, \qquad \tau_{\max} = \frac{1}{2\mu}. \tag{75}$$

As $\kappa(\theta^*) \geq 2\mu > 0$ across the entire interior, κ never approaches zero for $\mu > 0$; thus, Fisher-geometric softening ($\kappa \to 0$) does not occur in this model (Figure 4). Conversely, as θ^* approaches either boundary (0 or 1), the relaxation rate $\kappa(\theta^*)$ diverges, whereas the characteristic relaxation time $\tau = \kappa^{-1}$ tends to zero.

https://doi.org/10.3390/sym18121997

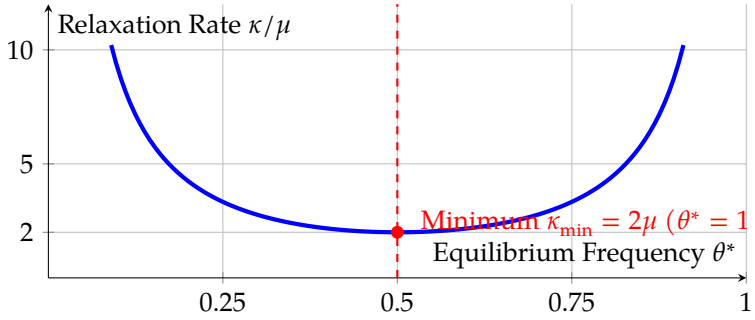

Figure 4. Normalized relaxation rate $\kappa(\theta^*)/\mu = [\theta^{*2} + (1-\theta^*)^2]/[\theta^*(1-\theta^*)]$ at the interior mutation–selection equilibrium $\theta^* \in (0,1)$. The rate reaches a strictly positive minimum $\kappa_{\min} = 2\mu$ at $\theta^* = 1/2$ (pure mutation) and diverges as $\theta^* \to 0, 1$.

9. Relation to Other Frameworks, Scope, and Extensions

The components assembled in this synthesis connect several established traditions in mathematical biology and statistics:

- *Information Geometry and Statistical Inference:* The Fisher metric $g_{AB} = \mathbb{E}_X[\partial_A \log p\, \partial_B \log p]$ quantifies local statistical distinguishability via $D_{\mathrm{KL}} = \frac{1}{2} ds_F^2 + O(|dX|^3)$ [1–4] and enters natural-gradient optimization [5,13]. In evolutionary applications, X^A parameterizes population states, rather than unknown inference parameters, and Fisher distance is model-dependent rather than an absolute biological distance.
- *Population Genetics and Evolutionary Game Theory:* On the categorical simplex, the Fisher metric induces the Shahshahani geometry [6–8], linking the replicator selection speed to fitness variance [9–12]. However, the same statistical manifold supports both gradient and non-gradient vector fields [14,16].
- *Thermodynamic Analogies and Scope:* The presence of a Fisher metric does not by itself establish a thermodynamic theory; thermodynamic potentials, conjugate state equations, and balance laws require additional physical postulates. Similarly, Fisher speed measures statistical deformation, rather than metabolic energy expenditure.
- *Extensions:* Future extensions include stochastic differential equations on $(\mathcal{M}_E, g_{AB})$ to incorporate genetic drift, joint population–environment manifolds $X^A = (p_1, \ldots, p_m, E^1, \ldots, E^k)$, and empirical estimation of Fisher trajectories from longitudinal population data.

Insights for Logit and Best-Response Adjustment Dynamics

As our framework separates the statistical metric g_{AB} from the evolutionary vector field F^A, it applies directly to adjustment rules beyond the replicator equation, yielding distinct geometric signatures for Logit and Best-Response dynamics on the simplex Δ^{m-1}:

1. *Logit (Smooth Best-Response) Dynamics:* Under logit choice with rationality parameter $\eta > 0$, population frequencies evolve according to

$$\dot{p}_i = \sigma_i(p) - p_i, \qquad \sigma_i(p) = \frac{\exp(\eta f_i(p))}{\sum_{j=1}^{m} \exp(\eta f_j(p))}. \tag{76}$$

Evaluating the squared Fisher–Shahshahani speed gives

$$v_F^2 = \sum_{i=1}^{m} \frac{(\sigma_i(p) - p_i)^2}{p_i} = \chi^2(\sigma(p) \,\|\, p), \tag{77}$$

showing that the instantaneous statistical velocity equals the Pearson χ^2-divergence between the target logit choice distribution $\sigma(\mathrm{p})$ and the current population state p. Unlike pure replicator dynamics, v_F^2 remains strictly positive at the boundaries ($p_i \to 0$)

because smooth exploration injects probability into unrepresented strategies ($\sigma_i > 0$). Moreover, in potential games where $f_i(p) = \partial_i U(p)$, logit dynamics minimizes the free-energy potential $\Phi_{\text{logit}}(p) = -U(p) + \eta^{-1} \sum_i p_i \ln p_i$ along mirror-descent trajectories [14], whereas non-potential games introduce rotational currents J^A around interior logit equilibria.

2. *Best-Response Dynamics:* In the deterministic limit $\eta \to \infty$, trajectories follow the differential inclusion

$$\dot{p}_i \in \text{BR}_i(p) - p_i, \tag{78}$$

where $\text{BR}(p) = \arg\max_{q \in \Delta^{m-1}} \sum_i q_i f_i(p)$. Whenever the population moves toward a unique pure best response e_k, the Fisher speed simplifies to

$$v_F^2 = \frac{(1-p_k)^2}{p_k} + \sum_{i \neq k} \frac{(-p_i)^2}{p_i} = \frac{1-p_k}{p_k}. \tag{79}$$

Thus, v_F^2 diverges as $p_k \to 0$ (invading a rare optimal strategy induces an arbitrarily large initial rate of statistical distinguishability) and vanishes linearly as $p_k \to 1$. Geometrically, best-response trajectories follow piecewise-linear rays toward simplex vertices and undergo non-smooth switching across indifference hyperplanes where the standard Jacobian operator J_B^A is undefined, requiring subdifferential stability analysis on (Δ^{m-1}, g_{ij}).

10. Conclusions

We present a unified information-geometric synthesis of evolutionary dynamics that explicitly separates the statistical representation of a population, the Riemannian geometry of statistical distinguishability, and the biological dynamical law governing evolutionary trajectories. Within this hierarchy, pure replicator dynamics satisfy $v_F^2 = \text{Var}_p(f)$, whereas general selection–mutation flows decompose v_F^2 into selection, mutation, and geometric cross-term contributions. When an evolutionary potential Φ_E exists, Fisher-natural-gradient dynamics obey the conditional dissipation identity $-d\Phi_E/dt = v_F^2$, and local relaxation and susceptibility near stable equilibria scale as κ_α^{-1} in terms of the Fisher-relative Hessian eigenvalues. When non-gradient currents are present—as in cyclic frequency-dependent games or asymmetric mutation regimes—potential dissipation breaks down and local stability must be evaluated via the full Jacobian of the evolutionary vector field. By keeping statistical geometry distinct from dynamical postulates, this framework provides a consistent geometric language across gradient and nonequilibrium evolutionary processes.

Funding: This research received no external funding.

Data Availability Statement: The data presented in this study are available on request from the corresponding author.

Conflicts of Interest: The author declares no conflicts of interest.

References

1. Rao, C.R. Information and the accuracy attainable in the estimation of statistical parameters. *Bull. Calcutta Math. Soc.* **1945**, *37*, 81–91.
2. Fisher, R.A. On the mathematical foundations of theoretical statistics. *Philos. Trans. R. Soc. Lond. Ser. A* **1922**, *222*, 309–368. [CrossRef]
3. Amari, S.-I. *Differential-Geometrical Methods in Statistics*; Lecture Notes in Statistics; Springer: Berlin/Heidelberg, Germany, 1985; Volume 28.
4. Amari, S.-I.; Nagaoka, H. *Methods of Information Geometry*; American Mathematical Society: Providence, RI, USA, 2000.

5. Amari, S.-I. *Information Geometry and Its Applications*; Springer: Tokyo, Japan, 2016.
6. Shahshahani, S. *A New Mathematical Framework for the Study of Linkage and Selection*; Memoirs of the American Mathematical Society; American Mathematical Society: Providence, RI, USA, 1979; Volume 17.
7. Akin, E. *The Geometry of Population Genetics*; Springer: Berlin/Heidelberg, Germany, 1979.
8. Harper, M. Information geometry and evolutionary game theory. *arXiv* **2009**, arXiv:0911.1383.
9. Frieden, B.R.; Plastino, A.; Soffer, B.H. Population genetics from an information perspective. *J. Theor. Biol.* **2001**, *208*, 49–64. [CrossRef] [PubMed]
10. Frank, S.A. Natural selection maximizes Fisher information. *J. Evol. Biol.* **2009**, *22*, 231–244. [CrossRef] [PubMed]
11. Frank, S.A. Natural selection. IV. The Price equation. *J. Evol. Biol.* **2012**, *25*, 1002–1019. [CrossRef] [PubMed]
12. Fisher, R.A. *The Genetical Theory of Natural Selection*; Clarendon Press: Oxford, UK, 1930.
13. Amari, S.-I. Natural gradient works efficiently in learning. *Neural Comput.* **1998**, *10*, 251–276. [CrossRef]
14. Hofbauer, J.; Sigmund, K. *Evolutionary Games and Population Dynamics*; Cambridge University Press: Cambridge, UK, 1998.
15. Chentsov, N.N. *Statistical Decision Rules and Optimal Inference*; Translations of Mathematical Monographs; American Mathematical Society: Providence, RI, USA, 1982; Volume 53.
16. Hofbauer, J. The selection mutation equation. *J. Math. Biol.* **1985**, *23*, 41–53. [CrossRef] [PubMed]

Disclaimer/Publisher's Note: The statements, opinions and data contained in all publications are solely those of the individual author(s) and contributor(s) and not of MDPI and/or the editor(s). MDPI and/or the editor(s) disclaim responsibility for any injury to people or property resulting from any ideas, methods, instructions or products referred to in the content.